




Integrin $\alpha 11\beta 1$ is expressed in breast cancer stroma and associates with aggressive tumor phenotypes

Hilde Ytre-Hauge Smeland^{1,2} , Cecilie Askeland^{1,3}, Elisabeth Wik^{1,3}, Gøril Knutsvik^{1,3}, Anders Molven^{3,4}, Reidunn J Edelman¹, Rolf K Reed², David J Warren⁵, Donald Gullberg², Linda Stuhr² and Lars A Akslen^{1,3*}

¹Centre for Cancer Biomarkers CCBIO, Department of Clinical Medicine, University of Bergen, Bergen, Norway

²Centre for Cancer Biomarkers CCBIO, Department of Biomedicine, University of Bergen, Bergen, Norway

³Department of Pathology, Haukeland University Hospital, Bergen, Norway

⁴Gade Laboratory for Pathology, Department of Clinical Medicine, University of Bergen, Bergen, Norway

⁵Department of Medical Biochemistry, Oslo University Hospital, Oslo, Norway

*Correspondence: Lars A Akslen, Centre for Cancer Biomarkers CCBIO, Department of Clinical Medicine, Section for Pathology, University of Bergen, Haukeland University Hospital, N-5021 Bergen, Norway. E-mail: lars.akslen@uib.no

Abstract

Cancer-associated fibroblasts are essential modifiers of the tumor microenvironment. The collagen-binding integrin $\alpha 11\beta 1$ has been proposed to be upregulated in a pro-tumorigenic subtype of cancer-associated fibroblasts. Here, we analyzed the expression and clinical relevance of integrin $\alpha 11\beta 1$ in a large breast cancer series using a novel antibody against the human integrin $\alpha 11$ chain. Several novel monoclonal antibodies against the integrin $\alpha 11$ subunit were tested for use on formalin-fixed paraffin-embedded tissues, and Ab 210F4B6A4 was eventually selected to investigate the immunohistochemical expression in 392 breast cancers using whole sections. mRNA data from METABRIC and co-expression patterns of integrin $\alpha 11$ in relation to α SMA and cytokeratin-14 were also investigated. Integrin $\alpha 11$ was expressed to varying degrees in spindle-shaped cells in the stroma of 99% of invasive breast carcinomas. Integrin $\alpha 11$ co-localized with α SMA in stromal cells, and with α SMA and cytokeratin-14 in breast myoepithelium. High stromal integrin $\alpha 11$ expression (66% of cases) was associated with aggressive breast cancer features such as high histologic grade, increased tumor cell proliferation, ER negativity, HER2 positivity, and triple-negative phenotype, but was not associated with breast cancer specific survival at protein or mRNA levels. In conclusion, high stromal integrin $\alpha 11$ expression was associated with aggressive breast cancer phenotypes.

Keywords: integrin $\alpha 11\beta 1$; monoclonal antibody; breast cancer; cancer associated fibroblasts; myoepithelial cells; clinico-pathologic features

Received 13 June 2019; Revised 5 September 2019; Accepted 16 September 2019

Conflict of interest statement: HYHS, RKR, DG and LAA are named as inventors on a patent regarding the 210F4B6A4 monoclonal antibody, filed by the University of Bergen, Norway.

Introduction

Breast cancer is a heterogeneous disease developed from genetically altered mammary epithelial cells, and there is a complex interplay between tumor cells and the surrounding tumor microenvironment (TME). The TME consists of various stromal cells, the extracellular matrix (ECM) scaffold, and the interstitial fluid, and both cellular and noncellular components have been shown to play an active role in tumor development, progression and metastasis [1]. Features of the TME contribute to clinically relevant variations in breast

cancer phenotypes and have also been shown to predict patient outcome [2,3].

Integrins are transmembrane cell-surface receptors crucial for bidirectional communication between cells and the surrounding ECM [4]. The collagen receptor integrin $\alpha 11\beta 1$ has emerged as a potentially important marker which is upregulated in fibroblasts during their differentiation into an activated phenotype [5–7]. Activated fibroblasts in the TME, termed cancer-associated fibroblasts (CAFs), constitute an abundant stromal cell type, especially in tumors with high stromal content such as pancreatic and breast carcinomas [1,8].

Accumulating data suggest the existence of diverse CAF subtypes, which differ in their biological functions, source of origin and expression of various markers [9–14]. Different fibroblasts may vary in their proliferative, secretory and contractile abilities and, most importantly, their influence on tumor growth and progression [9–14].

Integrin $\alpha 11\beta 1$ contributes to fibroblast function in wound healing, fibrosis and in different tumor models (reviewed in Zeltz and Gullberg [5]), binds to fibrillar collagen [15], and has been linked to collagen reorganization [5,15] and tumor interstitial fluid pressure [16,17]. *In vivo*, stromal integrin $\alpha 11$ -deficiency reduced the growth of triple-negative breast cancer [16] and prostate cancer xenografts [18], and reduced primary tumor growth [19,20] and metastasis [20] in lung cancer xenografts models. Thus, integrin $\alpha 11\beta 1$ could potentially represent a novel marker for a tumor-supportive subtype of CAFs and thereby play an important role in breast cancer progression.

The lack of reliable anti-human integrin $\alpha 11$ antibodies has limited the investigation of integrin $\alpha 11$ in retrospective studies using formalin-fixed and paraffin-embedded (FFPE) tumor material. We here present for the first time a study of integrin $\alpha 11$ expression in a large human breast cancer cohort with long-term follow-up, using a new in-house antibody specific for the human integrin $\alpha 11$ chain, aiming to investigate the expression of integrin $\alpha 11$ in human breast cancer, associations with aggressive phenotypes, as well as potential prognostic impact.

Materials and methods

Anti-human integrin $\alpha 11$ antibodies

Mouse monoclonal antibodies reactive to the extracellular domain of the integrin $\alpha 11$ subunit were generated by NanoTools (Teningen, Germany) for CCBIO (Centre of Cancer Biomarkers, University of Bergen, Bergen, Norway) as described in [21] and conducted in accordance with the German Animal Welfare Act and approved by the local German Authorities (RP Freiburg, AZ35/9185.82/I-13/03). In brief, mice were immunized with soluble human integrin $\alpha 11\beta 1$. Primary hybridoma screening was performed as described in [21]. In brief, selected hybridomas were reactive to C2C12- $\alpha 11$ cells, but not to C2C12, C2C12- $\alpha 2$ cells or A431 (expressing integrin $\beta 1$ and a variety of integrin α chains such as $\alpha 2$, $\alpha 3$, and $\alpha 5$, but not integrin $\alpha 11$ [22]). Secondary hybridoma screening was performed with flow cytometry and

western blotting as described elsewhere [23]. Anti-integrin $\alpha 11$ antibodies were then tested on FFPE tissue.

Mouse monoclonal antibodies reactive to the cytoplasmic domain of integrin $\alpha 11$ subunit were generated using the peptide H-CRREPGLDPTPKVLE-OH by Oslo University Hospital (Oslo, Norway). The peptide was custom-synthesized and conjugated to keyhole limpet hemocyanin (KLH) (Mimotopes, Clayton, Australia). BALB/c mice were immunized with the peptide-KLH conjugate and hybridomas constructed by fusion of splenocytes with the NS0 myeloma cell line (approved by the Norwegian Food Safety Authority with permit number 7903). Primary hybridoma screening was performed using antibody capture assays with biotinylated peptide (Biotin-SGSGRREPGLDPTPKVLE-OH) presented on streptavidin-coated 96-well microplates (Wallac Oy, Turku, Finland). Secondary screening was undertaken by western blotting and immunostaining of integrin $\alpha 11$ -positive and -negative cell lines and also frozen sections of pancreatic ductal adenocarcinoma (PDAC). D120.4 was then selected for use on FFPE tissue.

Monoclonal antibodies were purified from hybridoma culture supernatants by protein-A chromatography.

Cell culture

The integrin $\alpha 11$ - or $\alpha 2$ -overexpressing C2C12 cell lines, C2C12- $\alpha 11$, or C2C12- $\alpha 2$, were prepared as described previously [15], while U2OS and HEK293 were purchased from the American Type Culture Collection (ATCC, Manassas, VA, USA). All cells were cultured in DMEM with Glutamax (Gibco, Gaithersburg, MD, USA) supplemented with 10% fetal bovine serum, 100 units/ml of penicillin and 0.1 mg/ml of streptomycin (all from GE Healthcare, Chicago, IL, USA) under standard culture conditions (5% CO₂, 37 °C).

Western blotting and RT-qPCR

The cells were cultured to subconfluence and washed with PBS, lysed and collected in RIPA buffer (150 mM NaCl, 50 mM Tris base, 0.1% sodium dodecyl sulfate, 12 mM deoxycholate, 1% Nonidet-P40, 1% Triton X-100, pH 8) and supplemented with protease inhibitors (Roche Diagnostics, Basel, Switzerland). Protein concentration was determined by BCA assay (Bio-Rad, Hercules, CA, USA) after centrifugation. Of cleared lysates, 20 μ g were analyzed by SDS-PAGE and blotted onto PVDF membranes (Millipore, Burlington, MA, USA). The antibodies used were as

follows: mouse anti-human monoclonal integrin $\alpha 11$ antibody 210F4B6A4 (custom-made by NanoTools for CCBIO) (2.9 $\mu\text{g/ml}$), mouse anti-human monoclonal integrin $\alpha 11$ antibody D120.4 (custom-made by Oslo University Hospital) (2.8 $\mu\text{g/ml}$), rabbit anti-human polyclonal integrin $\alpha 11$ antibody [24] (1.9 $\mu\text{g/ml}$), anti- β -actin (Sigma–Aldrich, Steinheim, Germany) (1:5000), in addition to goat anti-rabbit and goat anti-mouse HRP-conjugated antibodies (Santa Cruz Biotechnology, Dallas, TX, USA) (1:5000). Chemiluminescence signals were developed using the ECL Western-blotting systems kit (GE Healthcare) and photographed using the ChemiDoc XRS device and the Quantity One 1-D Analysis Software (Bio-Rad).

RT-qPCR was performed as previously described [6]. In brief, total RNA was prepared from the cells using RNeasy Mini Kit (Qiagen, Hilden, Germany), and 1 μg RNA was used for reverse transcription to cDNA using iScript Reverse Transcription Supermix (Bio-Rad). qPCR mixtures were prepared with 20 ng of reverse-transcribed cDNA as a template, along with 0.5 μM of each primer, in a 10 μl qPCR using iQ SYBR Green Supermix (Bio-Rad). The qPCR was performed in a LightCycler 480 Instrument II (Roche Diagnostics). The reactions were prepared in triplicate for individual cDNA sample along with the negative controls where no cDNA was added for each primer pair. The experiment was repeated three times. The primers used were for target gene *ITGA11* and two references genes 18S rRNA and β -actin, and their sequences are shown in Table 1.

FFPE cell pellets

The cell lines were collected at subconfluence, centrifuged and washed with PBS. Plasma (Octaplas, Haukeland University Hospital, Bergen, Norway) and thrombin (Merck, Darmstadt, Germany) were added sequentially, and the pellets were fixed in 4% formaldehyde for 24 h and transferred to ethanol/xylene prior to embedding in paraffin wax.

Pancreatic ductal adenocarcinomas

Expression of the integrin $\alpha 11$ chain was investigated in corresponding cryosections and FFPE sections from

five different PDACs from a research biobank (Regional Ethical Committee approval 2013/1772) collected at Haukeland University Hospital [25].

Breast cancer series

Integrin $\alpha 11$ expression was investigated in a population-based cohort of 534 women diagnosed with primary invasive breast carcinoma (aged 50–69 at diagnosis) during 1996–2003 who resided in Hordaland County in Norway, as described previously [26]; treatment was given according to standard national guidelines at the time. Patients with distant metastatic disease at diagnosis were not included. Also, 14 cases were not included because of insufficient tissue in remaining blocks, leaving 520 cases for initial inclusion. Follow-up data were provided by the Norwegian Cause of Death Registry. Median follow-up time of survivors was 216 months (range 166–256), and last follow-up date was 30 June 2017. The study was approved by the Regional Committee for Medical and Health Sciences Research Ethics (REK #2014/1984), and was performed in accordance with the Declaration of Helsinki. In accordance with national ethics guidelines and procedures for such retrospective studies, all participants were contacted with written information on the study and asked to respond if they objected.

Immunohistochemistry

Cryosections of PDACs (4–5 μm) were fixed in acetone, rehydrated with PBS, and endogenous peroxidase activity was blocked with peroxidase block (Dako, K4007, Agilent, Santa Clara, CA, USA). Anti-integrin $\alpha 11$ 210F4B6A4 (0.39 $\mu\text{g/ml}$) was incubated in a humidity chamber overnight (4 $^{\circ}\text{C}$), followed by HRP-labeled anti-mouse antibody (Dako, K4001) (30 min), diaminobenzidine (DAB) (5 min) and hematoxylin (Dako, S2020) (3 min). A polyclonal antibody [24] and the new monoclonal antibody 203E3, recently demonstrated to be suitable for immunostaining of cryosections [21], were used as controls.

Immunohistochemical staining of FFPE tumor tissue was done on whole tissue sections (4–5 μm) mounted on poly-lysine coated glasses. The sections were baked

Table 1. Primer sequences for qPCR

Gene symbol	Forward primer	Reverse primer	Amplicon size (bp)
<i>ITGA11</i>	5'-CACGACATCAGTGGCAATAAG	5'-GACCCTCCCAGGTTGAGTT	132
<i>18S rRNA</i>	5'-GCAATTATCCCATGAACG	5'-GGGACTTAATCAACGCAAGC	68
<i>ACTB</i>	5'-GTGTGATGGTGGGAATGGGT	5'-TCTGGGTCATCATTACGGTTGG	240

at 56 °C for 48 h followed by cooling to room temperature (RT) (20 min), dewaxed with xylene/ethanol, and antigen retrieval was performed in Target Retrieval Solution pH 9 (Dako, K8010) (120 °C, 10 min) in a pressure cooker (Decloaking Chamber Plus, Biocare Medical, Pacheco, CA, USA). Staining was performed using a Dako autostainer Plus (Dako) with EnVision FLEX+ kit (Dako, K801021-2). Peroxidase Block was applied for 8 min, followed by incubation with anti-integrin α 11 210F4B6A4 (0.29 μ g/ml) (1 h RT), FLEX+ Mouse Linker (Dako, K8022) (15 min), FLEX+ HRP (20 min), DAB (5 min) and hematoxylin (3 min). Integrin α 11-positive and integrin α 11-negative FFPE cell pellets in addition to serial sections from one invasive breast carcinoma were used as biological controls. An anti-human IgG2b antibody was used as isotype control. Positive and negative controls were included in each run. Efforts were made to reduce the loss of tissue, such as baking prior to the IHC protocol, and using freshly cut sections and poly-lysine coated glasses.

For double and triple immunohistochemical staining, deparaffinization/rehydration and antigen retrieval were done as described above. Triple staining with antibodies against integrin α 11, α SMA and factor VIII (FVIII) was done on 20 FFPE invasive breast carcinomas with Ventana autostainer (Discovery Ultra, Ventana Medical systems, Tuscon, AZ, USA). After peroxidase block (Roche Diagnostics, 760–4840) (8 min), the sections were incubated with anti-integrin α 11 210F4B6A4 (0.29 μ g/ml) (1 h RT), Omnimap anti-mouse HRP (Roche Diagnostics, 760–4310) (16 min) and amplification with Amp HQ kit (Roche Diagnostics, 760–052) (20 min) and anti-HQ HRP (Roche Diagnostics, 760–4602) (16 min) following visualization with teal (Roche Diagnostics, 760–247) (32 + 16 min). The sections were denaturated in CC2 (Ventana, 950–243) (8 min 100 °C), and incubated with anti- α SMA (Dako, M0851) (1:100, 36 °C 32 min), Ultramap-anti mouse AP (Roche Diagnostics, 760–4312) (16 min) and visualized with yellow (Roche Diagnostics, 760–239) (44 min). After another denaturation with reaction buffer (Ventana, 95–300) (95 °C 20 min), the sections were incubated with anti-FVIII (Dako, A0088) (1:1600, 1 h RT), Ultramap anti-rabbit HRP (Roche Diagnostics, 760–4315) (12 min) and then purple (Roche Diagnostics, 760–229) (20 min).

Double immunofluorescent staining with antibodies against integrin α 11 and cytokeratin-14 (CK14) was done on 15 FFPE invasive breast carcinomas. After antigen retrieval, the sections were incubated with PBS/1% BSA/0.1% TritonX-100, followed by anti-human integrin α 11 210F4B6A4 (1.5 μ g/ml) in

combination with anti-CK14 (Abcam, Cambridge, United Kingdom, 119695) (1:700) (1 h RT), and then Alexa Fluor[®] 594 goat anti-mouse IgG (AffiniPure, Jackson ImmunoResearch, West Grove, PA, USA, 115-585-062) (1:700) and Alexa Fluor[®] 488 goat anti-rabbit IgG (AffiniPure, 111-545-045) (1:700) (1 h RT). Mounting was done with ProLong[™] Gold Antifade Mountant with DAPI (ThermoFisher, Waltham, MA, USA, P36931) and results recorded using a Zeiss AxioScope microscope equipped with Colibri 7 light source, AxioCam 503 mono camera and Axiovision software.

Evaluation of staining

Breast cancer sections were examined blinded for patient characteristics and outcome by a senior breast cancer pathologist, LAA, and HYHS. Of 520 stained sections, 128 tumors were excluded from evaluation because of inadequate tissue remaining after the antigen retrieval procedure. Altogether 392 cases were evaluated for integrin α 11-positive staining by a staining index (SI) score (0–9) which was obtained by multiplying the score for intensity of staining (0 = absent, 1 = weak, 2 = moderate, or 3 = strong) by the score for percentage of fibrous stroma stained (<10% = 1, 10–50% = 2, >50% = 3) [27]. Only positive staining in the tumor stroma was scored, and areas with hemorrhage and necrosis were avoided. Intratumor heterogeneity of stromal integrin α 11 expression was also noted.

As there is no pre-established cut-off value for integrin α 11, the distribution and frequency histograms for SI were evaluated. As seen in supplementary material, Figure S1, there was a clear binary distribution, and the breast cancer cases were therefore separated into integrin α 11-low expression (SI 0–3 = 34%) and integrin α 11-high expression (SI 4–9 = 66%) by this distribution, corresponding to a cut-off value at the lower tertile.

Gene expression data sets

Gene expression microarray data generated by the Molecular Taxonomy of Breast Cancer International Consortium (METABRIC) were included for analyses of *ITGA11* mRNA expression across breast cancer molecular subtypes and its relation to survival (discovery and validation cohorts) [28]. Cases of the normal-like molecular subtype were excluded, leaving $n = 939$ and $n = 843$ for analyses in the two cohorts. Two *ITGA11* probes were present in the METABRIC data. The max probe expression value was selected for

analyses [29]. Lower tertile was applied as cut-off, corresponding to the cut-off level of the protein staining.

Statistical analyses

Associations between categorical data were estimated using the Pearson's chi-square test and OR were computed. Differences in integrin $\alpha 11$ protein and mRNA expression across molecular subgroups were tested by Kruskal–Wallis test. Results were accepted as statistically significant when $p < 0.05$ (two-sided). Univariate survival data were analyzed by the Kaplan–Meier method, with death from breast cancer as end-point (time in months from diagnosis until death from breast cancer), and the significance determined by the log-rank test. Statistical analyses were performed using the IBM SPSS Statistics for Windows, Version 25.0 (IBM Corp, Armonk, NY, USA).

Results

Antibody specificity

As lack of reliable anti-human integrin $\alpha 11$ antibodies has limited the investigation of integrin $\alpha 11$ on FFPE tumor material, several novel monoclonal antibodies specific for human integrin $\alpha 11$ chain were generated and tested on FFPE tissues before use on the breast cancer cohort. Hybridoma screening and antibody characterization are demonstrated in [21,23], respectively. In brief, clones specific to integrin $\alpha 11$ chain, but not to other integrin subunits, such as integrin $\beta 1$ and $\alpha 2$, were chosen. Furthermore, the specificity of both 210F4B6A4 and D120.4 was validated by western blotting of cell lysates, and a polyclonal antibody was used as control [24]. Both clone 210F4B6A4 and D120.4 verified high expression of integrin $\alpha 11$ in C2C12- $\alpha 11$ cells and no expression in C2C12- $\alpha 2$ cells (Figure 1A). The human osteosarcoma cell line, U2OS, showed low integrin $\alpha 11$ expression while the human embryonic kidney cell line, HEK293, was negative for integrin $\alpha 11$ (Figure 1A). RT-qPCR confirmed the expression levels of integrin $\alpha 11$ in these cell lines (Figure 1B).

The clones were tested on FFPE material, and it became evident that high temperature was crucial to unmask the antigen. Extensive testing of different protocols was done to find the most gentle antigen retrieval protocol with high sensitivity. Several antibodies showed distinct staining on FFPE tissue, including 210F4B6A4 and D120.4. As 210F4B6A4

showed markedly strongest staining on FFPE tissue, this antibody was used for further analyses. Staining of FFPE cell pellets shows the validity of 210F4B6A4 on FFPE material (Figure 1C). Since other anti-integrin $\alpha 11$ antibodies have been shown to lack specificity on FFPE tissue, a positive reagent control was not applicable. Integrin $\alpha 11$ has recently been shown to be highly upregulated in PDAC [21], and corresponding cryo- and FFPE sections from the same PDACs were used in the calibration of the IHC protocol, where the polyclonal integrin $\alpha 11$ antibody and 203E3 [21] were used as a control for the cryosections. After optimizing the antigen retrieval protocol on FFPE sections from cell pellets, PDACs and invasive breast carcinomas, similar intensity and expression pattern were seen in corresponding cryo- and FFPE sections from five different PDACs (one representative of five different tumors is shown in Figure 1D). These sections were then used as biological controls. To exclude run-to-run variability, serial sections from five FFPE invasive breast carcinomas were stained.

Integrin $\alpha 11$ is expressed in fibroblast-like cells in breast cancer stroma

Positive staining was mainly seen as a fibrillar staining pattern in the breast cancer stroma (Figure 2A–I and see supplementary material, Figure S2A–I). Of note, cells positive for integrin $\alpha 11$ were mainly spindle-shaped, fibroblast-like cells, and the staining was often markedly accentuated in direct proximity to the cancer cells, indicating a 'border' between the epithelial component and the ECM (Figure 2B,D,E,G–I and see supplementary material, Figure S2A,B and D–F). In addition to this fibrillar stromal positivity, membrane staining of some of the breast myoepithelial cells was also seen (Figure 3A–I).

Integrin $\alpha 11$ was expressed in spindle-shaped stromal cells in 389 of 392 cases that were included for evaluation (99%). The stromal staining was markedly heterogeneous in 62% of the cases with an uneven distribution of integrin $\alpha 11$ expression (see supplementary material, Figure S3). Most of these heterogeneous cases showed highest integrin $\alpha 11$ expression in the central parts of the tumor with gradual loss of expression towards the invasive front (see supplementary material, Figure S3). Integrin $\alpha 11$ expression was most often weak in areas showing immune cell infiltration (see supplementary material, Figure S2B), and fibrotic, ECM-rich tissue was often positive for integrin $\alpha 11$ (see supplementary material, Figure S2C). No convincing staining of tumor cells was observed, not even

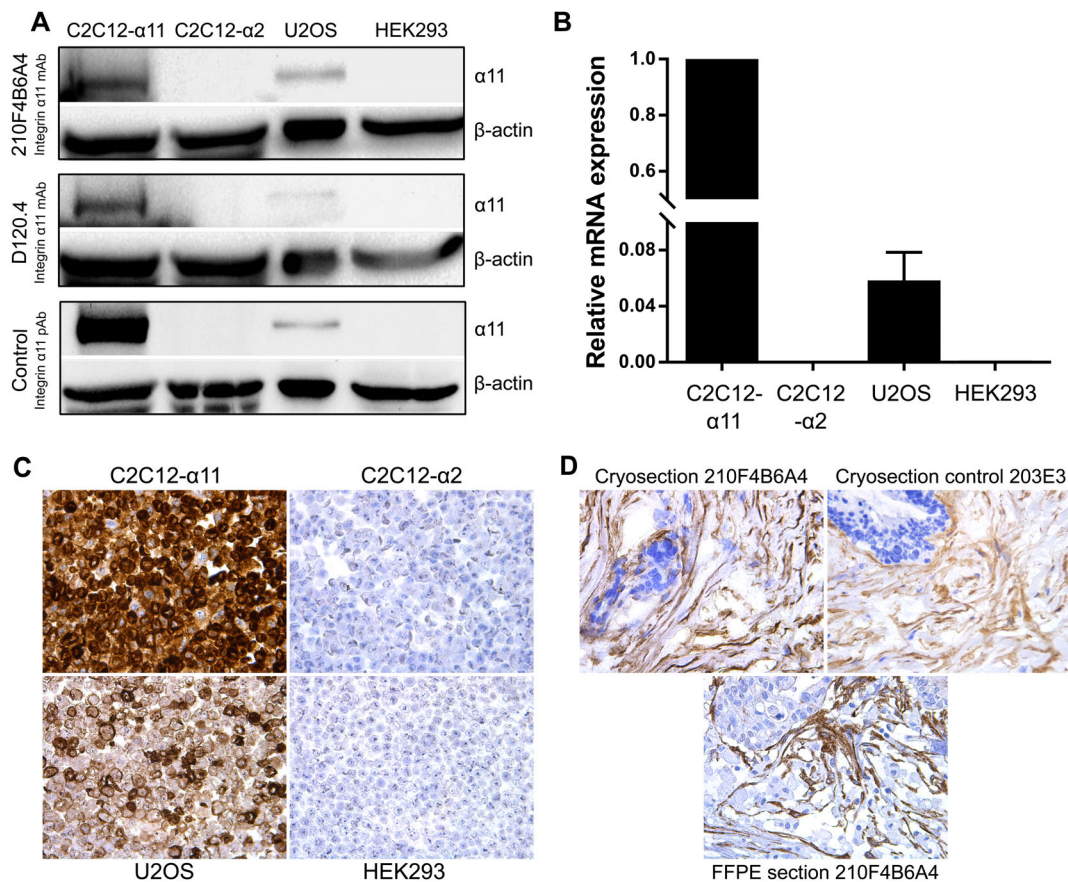


Figure 1. Validation of monoclonal antibodies against the integrin $\alpha 11$ subunit. Integrin $\alpha 11$ -positive cell lines (C2C12- $\alpha 11$ and U2OS) and integrin $\alpha 11$ -negative cell lines (C2C12- $\alpha 2$ and HEK293) were used to validate the monoclonal antibodies. Western blots show only expression of integrin $\alpha 11$ in cell lysates from integrin $\alpha 11$ -positive cells using the monoclonal antibodies (mAbs) 210F4B6A4 and D120.4 where a polyclonal antibody (pAb) was used as control (A). Comparison of mRNA expression of integrin $\alpha 11$ by RT-qPCR (B). *ITGA11* expression level is presented as the fold change in each cell line relative to C2C12- $\alpha 11$. Each column represents the average fold change from three experiments, and error bar indicates standard deviation. Staining with 210F4B6A4 of FFPE cell pellets confirmed the validity on FFPE material (C). Cases of pancreatic ductal adenocarcinoma stained with 210F4B6A4 showed similar stromal expression pattern in corresponding cryosections and FFPE sections; images from one representative tumor are shown in (D). 203E3 was used as control for the cryosections. Magnification: $\times 400$.

in invasive breast carcinomas with basal-like features (see supplementary material, Figure S2G–I).

Integrin $\alpha 11$ co-localizes with α SMA in fibroblast-like cells and with α SMA and cytokeratin-14 in breast myoepithelium

To further characterize the expression of integrin $\alpha 11$, we investigated its expression in relation to α SMA, CK14, and FVIII in invasive breast carcinomas. Integrin $\alpha 11$ and α SMA expression showed a clear co-localization in stromal spindle-shaped cells (Figure 2D–F), but spindle-shaped cells only positive for one of the markers were also observed (Figure 2F).

α SMA-positive, integrin $\alpha 11$ -negative fibroblasts were more prevalent than integrin $\alpha 11$ -positive, α SMA-negative fibroblasts. A minority of the vessels showed weak integrin $\alpha 11$ expression.

Furthermore, integrin $\alpha 11$ expression was observed in breast myoepithelial cells associated with ductal carcinoma *in situ* (DCIS), where it co-localized with α SMA (Figure 3E–F) and CK14 (Figure 3G–I). Integrin $\alpha 11$ -positive myoepithelial cells were more frequent and with higher intensity in DCIS (Figure 3B–C, E–F, and G–I) compared to benign-looking breast tissues where integrin $\alpha 11$ was mostly negative (Figure 3D). Nevertheless, positive integrin $\alpha 11$ staining was also observed in a small minority of

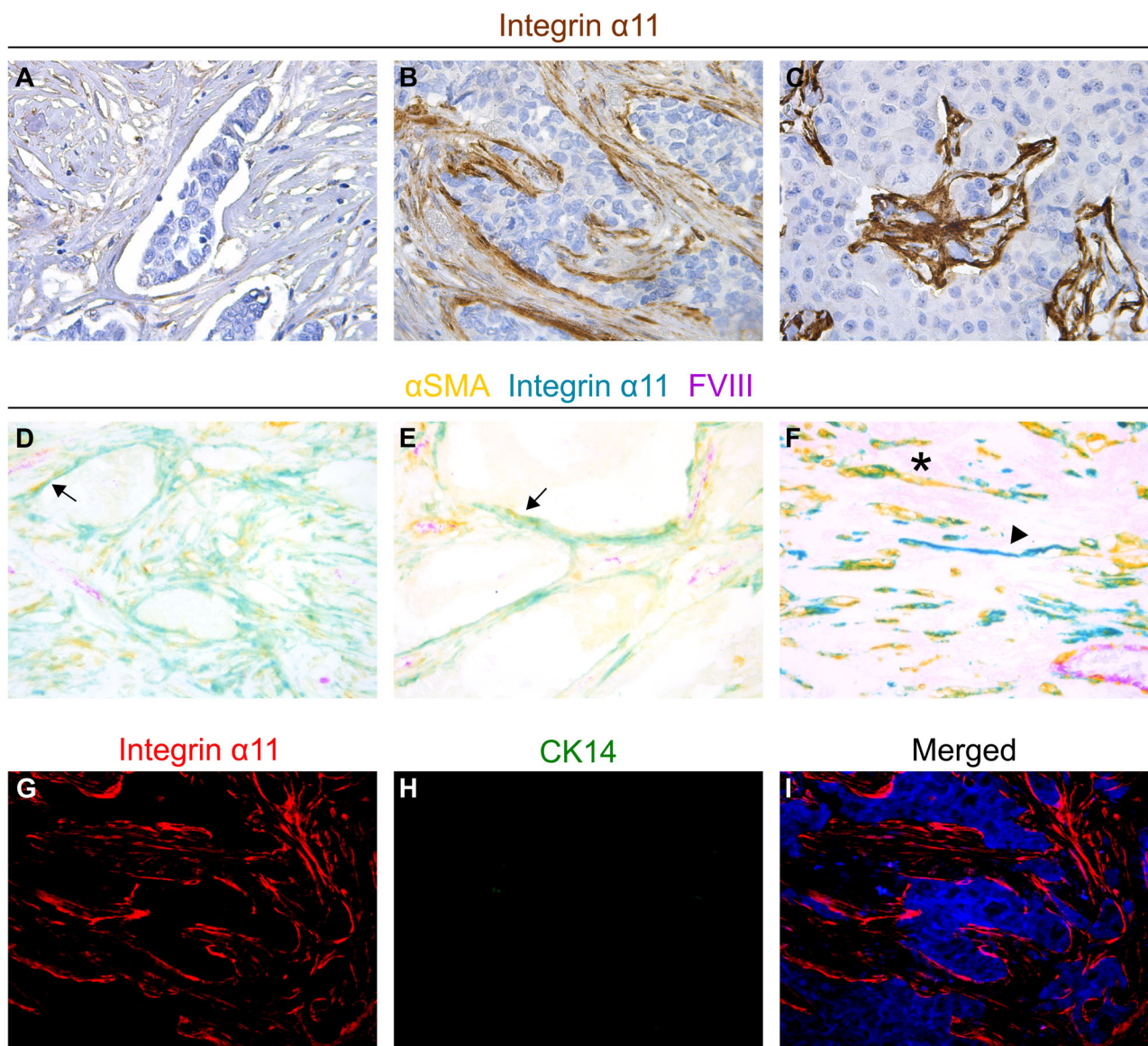


Figure 2. Integrin $\alpha 11$ is expressed in fibroblast-like cells in breast cancer stroma. Integrin $\alpha 11$ expression in spindle-shaped cells in the stroma of different invasive human breast carcinomas by IHC with 210F4B6A4. Different levels of integrin $\alpha 11$ expression are shown in (A–C) (A; low intensity, B; medium strong intensity and C; strong intensity). (D–F) show triple staining of α SMA (yellow), integrin $\alpha 11$ (teal), and FVIII (purple) where co-localization of α SMA and integrin $\alpha 11$ appears green. Note that both integrin $\alpha 11$ and α SMA are expressed in spindle-shaped stromal cells, but do not completely co-localize. Examples of double-positive spindle-shaped cells are marked with arrows, while one integrin $\alpha 11$ -positive/ α SMA-negative cell is marked with an arrowhead and one integrin $\alpha 11$ -negative/ α SMA-positive cell marked with an asterisk. (G–I) show immunofluorescent double staining of integrin $\alpha 11$ (red), CK14 (green) and DAPI (blue) of one invasive breast carcinoma. Note the strong integrin $\alpha 11$ expression in direct proximity to the tumor cells seen in (B), (D), (E), and (J–L), and that this border is negative for CK14, indicating that this is not flattened integrin $\alpha 11$ -positive breast myoepithelium. Magnification: $\times 400$ and $\times 200$.

histologically benign ducts (Figure 3A). Interestingly, Figure 2G–I and see supplementary material, Figure S2D–F, demonstrate that the accentuated integrin $\alpha 11$ expression in spindle-shaped cells near

tumor cells noted above probably represents tightly associated fibroblasts, and not myoepithelial cells, as these cells are negative for the myoepithelial marker CK14.

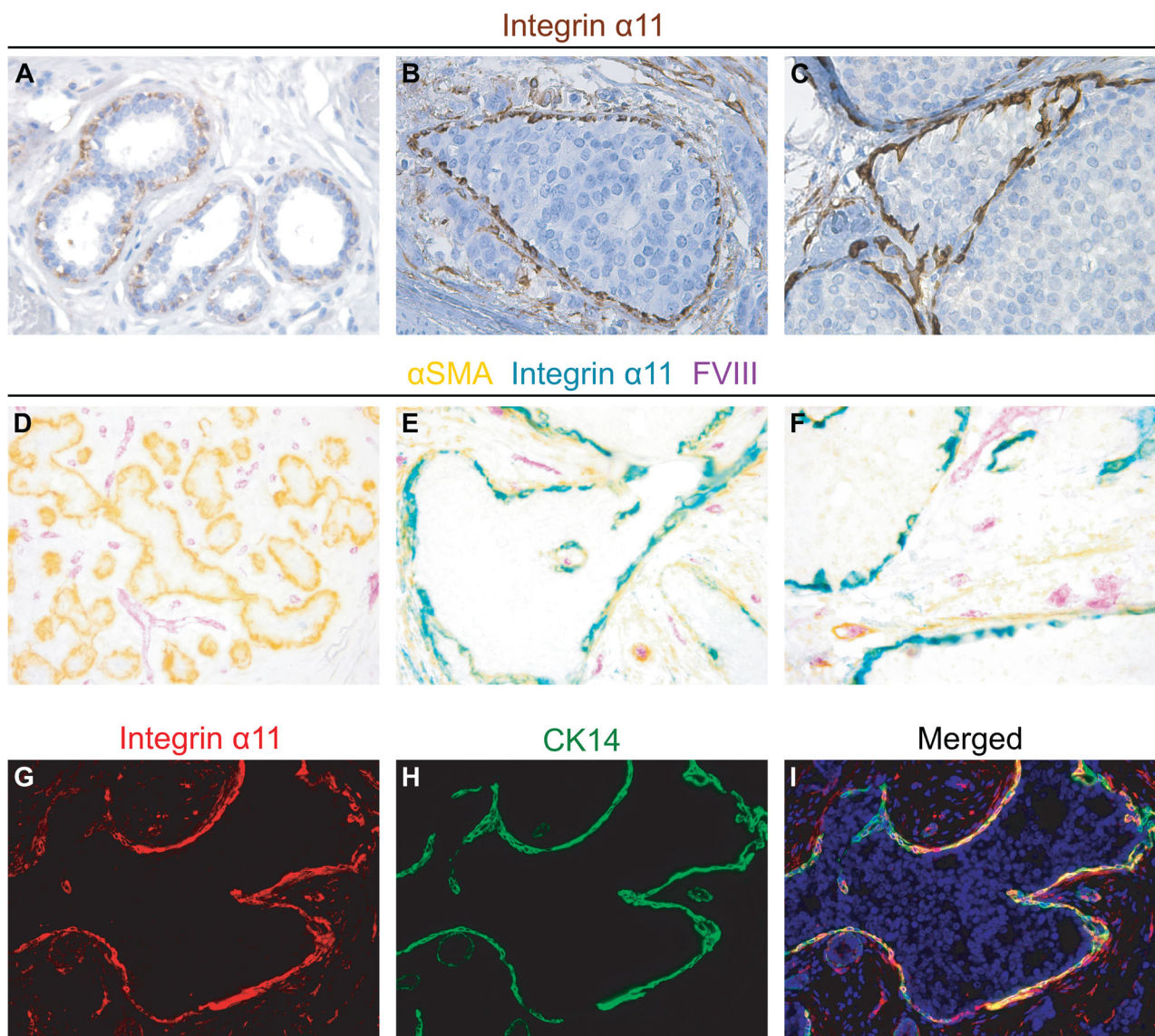


Figure 3. Integrin α 11 is expressed in a subgroup of breast myoepithelial cells. (A–C) show single staining of integrin α 11 with weak myoepithelial integrin α 11 expression in benign-appearing ducts (A) and high myoepithelial integrin α 11 expression in DCIS lesions (B and C). (D–F) show triple staining of α SMA (yellow), integrin α 11 (teal), and FVIII (purple) where co-localization of α SMA and integrin α 11 appears green; (D) shows terminal ducts and lobular units outside an invasive breast carcinoma with α SMA-positive, integrin α 11-negative myoepithelial cells, while (E–F) show co-localization of myoepithelial integrin α 11 and α SMA in DCIS lesions. (G–I) shows immunofluorescent double staining of integrin α 11 (red), CK14 (green) and DAPI (blue) of one DCIS lesion with co-localization of integrin α 11 and CK14 in myoepithelial cells. IHC with 210F4B6A4. Magnification: $\times 400$ and $\times 200$.

High integrin α 11 expression is associated with features of aggressive breast cancer

Integrin α 11 protein expression in stromal, spindle-shaped cells was quantified by SI score (0–9), obtained by multiplying the score for intensity of staining by the score for percentage of fibrous stroma stained. In total, 258 cases (66%) showed

high integrin α 11 protein expression (SI 4–9), whereas 134 cases (34%) showed low expression (SI 0–3). While invasive carcinoma of no special type, previously named invasive ductal carcinoma, was associated with high integrin α 11 protein expression, invasive lobular carcinoma was associated with low integrin α 11 protein expression (Table 2).

Table 2. Associations between integrin $\alpha 11$ protein expression and clinico-pathological variables

Variables	$\alpha 11$ low ($n = 134$)	$\alpha 11$ high ($n = 258$)	OR (95% CI)	P value*
	n (%)	n (%)		
Ductal carcinoma				<0.001
No	37 (58)	27 (42)	1	
Yes	97 (30)	231 (70)	3.3 (1.9–5.7)	
Lobular carcinoma				<0.001
Yes	27 (67)	13 (33)	1	
No	107 (30)	245 (70)	4.8 (2.4–9.6)	
Histologic grade				<0.001
Grade 1–2	125 (40)	190 (60)	1	
Grade 3	9 (12)	68 (88)	5.0 (2.4–10.3)	
Tumor diameter				0.96
≤ 2 cm	98 (34)	188 (66)	1	
> 2 cm	36 (34)	70 (66)	1.0 (0.6–1.6)	
Mitotic count ^{†,‡}				<0.001
Low count ($\leq 5.5/\text{mm}^2$)	117 (43)	158 (57)	1	
High count ($> 5.5/\text{mm}^2$)	16 (14)	98 (86)	4.5 (2.5–8.1)	
Lymph node status				0.11
Negative	101 (37)	175 (63.4)	1	
Positive	32 (28)	82 (72)	1.5 (0.9–2.4)	
ER				0.001
Positive ($\geq 10\%$)	121 (38)	197 (62)	1	
Negative ($< 10\%$)	13 (18)	61 (82)	2.9 (1.5–5.5)	
PR				0.53
Positive ($\geq 10\%$)	91 (35)	167 (65)	1	
Negative ($< 10\%$)	43 (32)	91 (68)	1.2 (0.7–1.8)	
HER2 [§]				0.004
Negative	123 (37)	209 (63)	1	
Positive	10 (18)	47 (82)	2.7 (1.3–5.7)	
Ki67 [†]				<0.001
Low count ($\leq 31.5\%$)	111 (41)	163 (59)	1	
High count ($> 31.5\%$)	22 (19)	93 (81)	2.9 (1.7–4.9)	
Triple-negative				0.022
No	126 (36)	223 (64)	1	
Yes	8 (19)	35 (81)	2.5 (1.1–5.5)	
CK 5/6				0.001
Negative (SI = 0)	124 (38)	207 (62)	1	
Positive (SI > 0)	9 (16)	49 (84)	3.3 (1.5–6.9)	

n , number of patients; ER, estrogen receptor; PR, progesterone receptor; HER2, human epidermal growth factor receptor 2; CK 5/6, cytokeratin 5/6; SI: staining index.

*Pearson chi-square.

[†]Cut-off value by upper quartile.

[‡]Mitotic count: number of mitoses per mm^2 .

[§]HER2-positive cases: HER2 IHC3+ and HER2 IHC2+ cases with a HER2/Chr17 ratio by silver *in situ* hybridization ≥ 2.0 .

Furthermore, the expression of integrin $\alpha 11$ was significantly higher in the aggressive HER2-positive breast cancer subgroup both at protein and mRNA level (Figures 4A and 5A,C).

Using the lower tertile as cut-off value (SI 0–3 = 34% versus SI 4–9 = 66%), high integrin $\alpha 11$ protein expression was significantly associated with high histologic grade (OR 5.0), estrogen receptor (ER) negativity (OR 2.9), HER2 positivity (OR 2.7), triple-negative phenotype (OR 2.5) and high tumor cell proliferation by Ki-67 (OR 2.9) and mitotic count (OR 4.5) (Table 2). Furthermore, high integrin $\alpha 11$ protein expression was associated with the basal cell marker

CK5/6 (OR 3.3), but not with tumor diameter or lymph node metastasis (Table 2).

In univariate survival analyses, neither integrin $\alpha 11$ protein expression nor integrin $\alpha 11$ mRNA expression were significantly associated with breast cancer specific survival (Figures 4B and 5B,D). No significant associations between integrin $\alpha 11$ expression and breast cancer specific survival were found across different molecular breast cancer subgroups (see supplementary material, Figures S4–S6), except that high integrin $\alpha 11$ mRNA expression was found to be associated with reduced survival in the Luminal B subgroup in the METABRIC discovery cohort (see

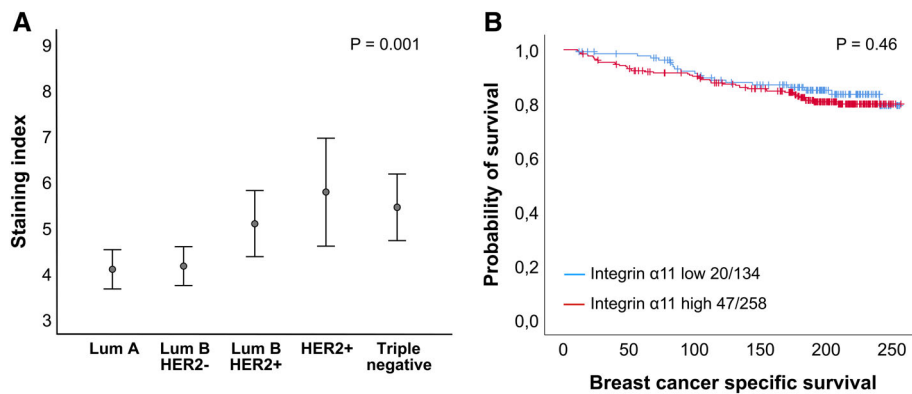


Figure 4. Integrin $\alpha 11$ protein expression in human breast cancer. Integrin $\alpha 11$ protein expression across molecular subtypes of breast cancer; data are presented as error-bars with 95% confidence interval of the mean, and P values by the Kruskal–Wallis test (A). Survival curve by the Kaplan–Meier method for stromal integrin $\alpha 11$ expression; breast cancer specific survival in months, and P value by log-rank test (B). For each category, the number of breast cancer deaths is given, followed by the total number of cases in each category.

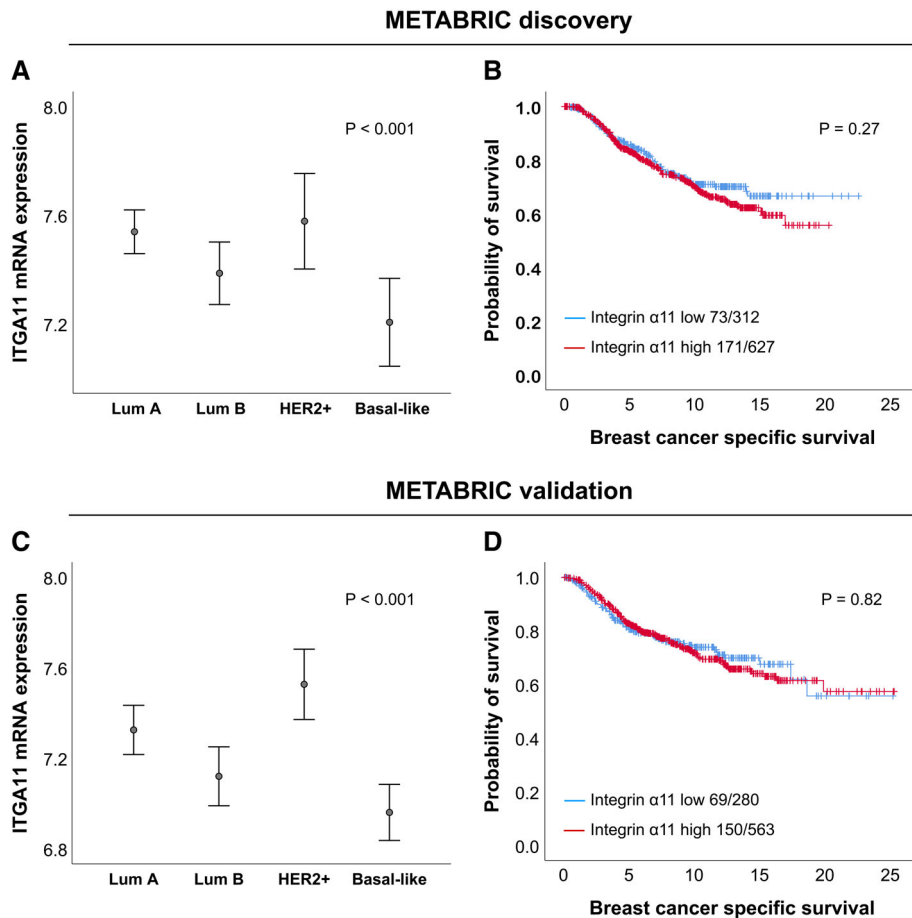


Figure 5. Integrin $\alpha 11$ mRNA expression in human breast cancer in the METABRIC discovery and validation datasets. Integrin $\alpha 11$ mRNA expression across molecular subtypes of breast cancer; data are presented as error-bars with 95% confidence interval of the mean, and P values by the Kruskal–Wallis test (A,C). Survival curves by the Kaplan–Meier method for integrin $\alpha 11$ mRNA expression; breast cancer specific survival in years, and P value by log rank test (B,D). For each category, the number of breast cancer deaths is given, followed by the total number of cases in each category.

supplementary material, Figure S5B), but this was not validated at the protein level or in the METABRIC validation cohort (see supplementary material, Figures S4B,C and S6B).

Discussion

Integrin $\alpha 11\beta 1$ has been shown experimentally to stimulate tumor growth and progression [16,17,19,20], and to be essential for fibroblast-matrix interactions [5,30]. Here, we present two new monoclonal mouse anti-human integrin $\alpha 11$ antibodies, 210F4B6A4 and D120.4, which bind to extracellular and intracellular epitopes of the integrin $\alpha 11$ subunit, respectively. We have established conditions for specific and reproducible integrin $\alpha 11$ staining of human FFPE tumor material with 210F4B6A4. In a large breast cancer cohort with long and complete follow-up, integrin $\alpha 11$ was found to be expressed to varying degrees in the stroma of 99% of the cases. In agreement with a tumor-supportive effect of integrin $\alpha 11\beta 1$, high integrin $\alpha 11$ expression was associated with more aggressive breast cancer phenotypes, even though integrin $\alpha 11$ expression was not significantly correlated to breast cancer specific survival.

Since existing anti-integrin $\alpha 11$ antibodies have been shown to lack specificity on FFPE material in our laboratory, we carefully developed and characterized novel antibodies. Since integrin $\alpha 2$ is one of the most similar integrin chains [24], and is also found expressed on fibroblasts [5], extra efforts were made to exclude cross-reactivity against this integrin subunit. The new monoclonal antibody 210F4B6A4 described herein binds specifically to the integrin $\alpha 11$ -chain under several conditions, including western blotting and immunostaining of FFPE material.

Although experimental studies have indicated a tumor-stimulating effect of integrin $\alpha 11\beta 1$ in different preclinical models [16,17,19,20], and integrin $\alpha 11\beta 1$ therefore has been suggested as a potential marker of a pro-tumorigenic CAF subset, few investigations have been performed on human tumor tissue due to lack of a reliable antibody for use on FFPE material. In the present study, investigating a breast cancer cohort of 392 patients, high integrin $\alpha 11$ expression in stromal spindle-shaped cells was significantly associated with high histologic grade, HER2 positivity, ER negativity, triple-negative phenotype and expression of the basal cell marker CK5/6, as well as high tumor cell proliferation by Ki-67 expression and mitotic count - all markers of aggressive breast cancer phenotypes.

Notably, integrin $\alpha 11$ was expressed at higher protein and mRNA levels in the aggressive HER2-positive subtype of breast cancer. In addition to existing pre-clinical data, these findings may indicate that integrin $\alpha 11$ -positive fibroblasts represent a subset of tumor-supportive breast CAFs. However, high integrin $\alpha 11$ protein and mRNA expression was not associated with survival. Similarly, Parajuli *et al* [31] did not find correlations between stromal integrin $\alpha 11$ expression and patient outcome in a series of head and neck cancers using cryosections from the tumor center.

The cellular expression of different integrins is not only subtype-specific, but is also dependent on tissue type and context [4,32,33]. In the case of integrin $\alpha 11\beta 1$, the expression appears to be restricted to a subgroup of fibroblasts and mesenchymal stem cells [5], but the characterization of expression in human tissue is so far limited. As there is a need to better characterize CAF heterogeneity and to identify markers that can help distinguish between tumor-supportive and tumor-suppressive CAFs, several IHC-based studies have used different markers to identify tumor-supportive breast CAFs, such as α SMA [34,35] and PDGFR β [36,37]. In the present study, we found that the integrin $\alpha 11$ subunit was expressed in fibroblast-like cells in the breast tumor stroma, and it predominantly co-localized with α SMA. Similarly, α SMA and integrin $\alpha 11$ have previously been found to co-localize in the tumor stroma of human head and neck cancers [31]. However, stromal spindle-shaped cells with expression of either integrin $\alpha 11$ or α SMA only were also observed in the present study, which may represent different subpopulations of CAFs ($\alpha 11$ +/ α SMA+, $\alpha 11$ +/ α SMA-, and $\alpha 11$ -/ α SMA+) with potential functional differences which should be investigated in future studies.

Normal mammary epithelium consists of an inner luminal and a surrounding myoepithelial cell layer [38]. Interestingly, integrin $\alpha 11$ was also found to be expressed on myoepithelial cells surrounding DCIS lesions, where it was found to co-localize with α SMA and CK14, common markers of breast myoepithelium. While α SMA and CK14 are general myoepithelial markers, integrin $\alpha 11$ myoepithelial expression appears to be more restricted, and was mainly detected in *in situ* lesions, with absent or very weak expression in benign-appearing lobules and ducts. While the myoepithelium of benign ducts is thought to act as an active tumor suppressor, accumulating data indicate that DCIS-associated myoepithelial cells show genetic, epigenetic and molecular changes compared to myoepithelium in benign tissue, and that their tumor-suppressive

function may be lost with DCIS progression [39,40]. As changes in myoepithelial cells have been suggested to be an important contribution in the transition from preinvasive to invasive cancer, the molecular differences in preinvasive lesions may represent markers for risk stratification or even targets for prevention of invasive breast cancer. Interestingly, upregulation of another integrin, integrin $\alpha\beta 6$, in breast myoepithelium, has been associated with poor patient outcome and shown to promote breast tumor proliferation experimentally [41]. Additional studies should address the role of myoepithelial integrin $\alpha 11$ expression in DCIS cohorts.

We observed fibrillar integrin $\alpha 11$ positivity which was clearly strongest in direct proximity to the tumor cells in the majority of breast cancer samples, and dual staining with CK14 demonstrated that these cells are probably not flattened myoepithelial cells. By the methods used in this study, we cannot exclude that such accentuated integrin $\alpha 11$ staining adjacent to cancer cells may represent a subset of the tumor cell population with a mesenchymal phenotype. Indeed, integrin $\alpha 11\beta 1$ has been suggested to be upregulated during epithelial-to-mesenchymal transition, as it was found to be part of a gene signature for some invading breast cancer cells *in vitro* [42], although this has not been confirmed in other models or at the protein level.

In conclusion, we have shown that the integrin $\alpha 11$ subunit is expressed in fibroblasts-like cells in invasive human breast carcinomas, and in myoepithelial cells in *in situ* lesions. High stromal integrin $\alpha 11$ expression was associated with aggressive breast cancer phenotypes, although integrin $\alpha 11$ mRNA and protein expression did not correlate with breast cancer specific survival. It will be of further interest to examine the expression of integrin $\alpha 11$ in relation to other CAF markers, and to study the functional role of integrin $\alpha 11$ -expressing subpopulations of breast CAFs.

Acknowledgements

The authors would like to thank Ning Lu (RT-qPCR, western blotting and immunofluorescence staining), Gerd Lillian Hallseth (immunohistochemistry) and Bendik Nordanger (histochemical work) for excellent technical assistance. This work was supported by the Research Council of Norway through its Centres of Excellence funding scheme, project number 223250, and by a Meltzer Fund Research Grant.

Author contributions statement

HYHS, RKR, and LAA contributed to the concept and design of the study. HYHS, RJE, and LAA planned and analyzed the IHC data. HYHS performed the experiments. DW produced the D120.4 antibody, and purified anti-integrin $\alpha 11$ antibodies from hybridoma culture supernatants. CA, EW, and GK contributed to collection and assembly of data from the patient materials. AM provided frozen and FFPE tissue sections of pancreatic ductal adenocarcinomas. EW collected and analyzed microarray mRNA data sets. HYHS, CA, and EW conducted statistical analyses. HYHS, RJE, RKR, DW, DG, LS, and LAA contributed to reagents/materials/analyses tools. HYHS and LAA wrote the manuscript with critical input from co-authors. All authors read and approved the final version of the manuscript.

References

1. Maman S, Witz IP. A history of exploring cancer in context. *Nat Rev Cancer* 2018; **18**: 359–376.
2. Nienhuis HH, Gaykema SB, Timmer-Bosscha H, et al. Targeting breast cancer through its microenvironment: current status of pre-clinical and clinical research in finding relevant targets. *Pharmacol Ther* 2015; **147**: 63–79.
3. Finak G, Bertos N, Pepin F, et al. Stromal gene expression predicts clinical outcome in breast cancer. *Nat Med* 2008; **14**: 518–527.
4. Barczyk M, Carracedo S, Gullberg D. Integrins. *Cell Tissue Res* 2010; **339**: 269–280.
5. Zeltz C, Gullberg D. The integrin-collagen connection – a glue for tissue repair? *J Cell Sci* 2016; **129**: 653–664.
6. Carracedo S, Lu N, Popova SN, et al. The fibroblast integrin $\alpha 11\beta 1$ is induced in a mechanosensitive manner involving activin A and regulates myofibroblast differentiation. *J Biol Chem* 2010; **285**: 10434–10445.
7. Talior-Volodarsky I, Connelly KA, Arora PD, et al. $\alpha 11$ integrin stimulates myofibroblast differentiation in diabetic cardiomyopathy. *Cardiovasc Res* 2012; **96**: 265–275.
8. Bussard KM, Mutkus L, Stumpf K, et al. Tumor-associated stromal cells as key contributors to the tumor microenvironment. *Breast Cancer Res* 2016; **18**: 84.
9. Ohlund D, Handly-Santana A, Biffi G, et al. Distinct populations of inflammatory fibroblasts and myofibroblasts in pancreatic cancer. *J Exp Med* 2017; **214**: 579–596.
10. Ozdemir BC, Pentcheva-Hoang T, Carstens JL, et al. Depletion of carcinoma-associated fibroblasts and fibrosis induces immunosuppression and accelerates pancreas cancer with reduced survival. *Cancer Cell* 2014; **25**: 719–734.
11. Rhim AD, Oberstein PE, Thomas DH, et al. Stromal elements act to restrain, rather than support, pancreatic ductal adenocarcinoma. *Cancer Cell* 2014; **25**: 735–747.

12. Costa A, Kieffer Y, Scholer-Dahirel A, *et al.* Fibroblast heterogeneity and immunosuppressive environment in human breast cancer. *Cancer Cell* 2018; **33**: 463–479.e410.
13. Barbazan J, Vignjevic DM. Cancer associated fibroblasts: is the force the path to the dark side? *Curr Opin Cell Biol* 2019; **56**: 71–79.
14. Kwa MQ, Herum KM, Brakebusch C. Cancer-associated fibroblasts: how do they contribute to metastasis? *Clin Exp Metastasis* 2019; **36**: 71–86.
15. Tiger CF, Fougousse F, Grundstrom G, *et al.* $\alpha 11\beta 1$ integrin is a receptor for interstitial collagens involved in cell migration and collagen reorganization on mesenchymal nonmuscle cells. *Dev Biol* 2001; **237**: 116–129.
16. Smeland HY, Lu N, Karlsen TV, *et al.* Stromal integrin $\alpha 11\beta 1$ -deficiency reduces interstitial fluid pressure and perturbs collagen structure in triple-negative breast xenograft tumors. *BMC Cancer* 2019; **19**: 234.
17. Lu N, Karlsen TV, Reed RK, *et al.* Fibroblast $\alpha 11\beta 1$ integrin regulates tensional homeostasis in fibroblast/A549 carcinoma heterospheroids. *PLoS One* 2014; **9**: e103173.
18. Reigstad I, Smeland HY, Skogstrand T, *et al.* Stromal integrin $\alpha 11\beta 1$ affects RM11 prostate and 4T1 breast Xenograft tumors differently. *PLoS One* 2016; **11**: e0151663.
19. Zhu CQ, Popova SN, Brown ER, *et al.* Integrin $\alpha 11$ regulates IGF2 expression in fibroblasts to enhance tumorigenicity of human non-small-cell lung cancer cells. *Proc Natl Acad Sci U S A* 2007; **104**: 11754–11759.
20. Navab R, Strumpf D, To C, *et al.* Integrin $\alpha 11\beta 1$ regulates cancer stromal stiffness and promotes tumorigenicity and metastasis in non-small cell lung cancer. *Oncogene* 2016; **35**: 1899–1908.
21. Zeltz C, Alam J, Liu H, *et al.* $\alpha 11\beta 1$ integrin is induced in a subset of cancer-associated fibroblasts in desmoplastic tumor stroma and mediates in vitro cell migration. *Cancers (Basel)* 2019; **11**: p.ii: E765.
22. Pidgeon GP, Tang K, Cai YL, *et al.* Overexpression of platelet-type 12-lipoxygenase promotes tumor cell survival by enhancing $\alpha (v)\beta 3$ and $\alpha (v)\beta 5$ integrin expression. *Cancer Res* 2003; **63**: 4258–4267.
23. Erusappan P, Alam J, Lu N, *et al.* Integrin $\alpha 11$ cytoplasmic tail is required for FAK activation to initiate 3D cell invasion and ERK-mediated cell proliferation. *Sci Rep* 2019; **9**: 15283.
24. Velling T, Kusche-Gullberg M, Sejersen T, *et al.* cDNA cloning and chromosomal localization of human $\alpha (11)$ integrin. A collagen-binding, I domain-containing, $\beta (1)$ -associated integrin α -chain present in muscle tissues. *J Biol Chem* 1999; **274**: 25735–25742.
25. El Jellas K, Hoem D, Hagen KG, *et al.* Associations between ABO blood groups and pancreatic ductal adenocarcinoma: influence on resection status and survival. *Cancer Med* 2017; **6**: 1531–1540.
26. Knutsvik G, Stefansson IM, Aziz S, *et al.* Evaluation of Ki67 expression across distinct categories of breast cancer specimens: a population-based study of matched surgical specimens, Core needle biopsies and tissue microarrays. *PLoS One* 2014; **9**: e112121.
27. Straume O, Akslen LA. Alterations and prognostic significance of p16 and p53 protein expression in subgroups of cutaneous melanoma. *Int J Cancer* 1997; **74**: 535–539.
28. Curtis C, Shah SP, Chin SF, *et al.* The genomic and transcriptomic architecture of 2,000 breast tumours reveals novel subgroups. *Nature* 2012; **486**: 346–352.
29. Subramanian A, Tamayo P, Mootha VK, *et al.* Gene set enrichment analysis: a knowledge-based approach for interpreting genome-wide expression profiles. *Proc Natl Acad Sci U S A* 2005; **102**: 15545–15550.
30. Schulz JN, Plomann M, Sengle G, *et al.* New developments on skin fibrosis – essential signals emanating from the extracellular matrix for the control of myofibroblasts. *Matrix Biol* 2018; **68–69**: 522–532.
31. Parajuli H, Teh MT, Abrahamsen S, *et al.* Integrin $\alpha 11$ is overexpressed by tumour stroma of head and neck squamous cell carcinoma and correlates positively with α smooth muscle actin expression. *J Oral Pathol Med* 2017; **46**: 267–275.
32. Hamidi H, Ivaska J. Every step of the way: integrins in cancer progression and metastasis. *Nat Rev Cancer* 2018; **18**: 532–547.
33. Hamidi H, Pietila M, Ivaska J. The complexity of integrins in cancer and new scopes for therapeutic targeting. *Br J Cancer* 2016; **115**: 1017–1023.
34. Surowiak P, Murawa D, Materna V, *et al.* Occurrence of stromal myofibroblasts in the invasive ductal breast cancer tissue is an unfavourable prognostic factor. *Anticancer Res* 2007; **27**: 2917–2924.
35. Amornsapak K, Jamjuntra P, Warnnissorn M, *et al.* High ASMA (+) fibroblasts and low cytoplasmic HMGB1(+) breast cancer cells predict poor prognosis. *Clin Breast Cancer* 2017; **17**: 441–452.e442.
36. Paulsson J, Ryden L, Strell C, *et al.* High expression of stromal PDGFR β is associated with reduced benefit of tamoxifen in breast cancer. *J Pathol Clin Res* 2017; **3**: 38–43.
37. Paulsson J, Sjoblom T, Micke P, *et al.* Prognostic significance of stromal platelet-derived growth factor β -receptor expression in human breast cancer. *Am J Pathol* 2009; **175**: 334–341.
38. Sirka OK, Shamir ER, Ewald AJ. Myoepithelial cells are a dynamic barrier to epithelial dissemination. *J Cell Biol* 2018; **217**: 3368–3381.
39. Rakha EA, Miligy IM, Gorringer KL, *et al.* Invasion in breast lesions: the role of the epithelial-stroma barrier. *Histopathology* 2018; **72**: 1075–1083.
40. Allen MD, Marshall JF, Jones JL. $\alpha (v)\beta 6$ expression in myoepithelial cells: a novel marker for predicting DCIS progression with therapeutic potential. *Cancer Res* 2014; **74**: 5942–5947.
41. Allen MD, Thomas GJ, Clark S, *et al.* Altered microenvironment promotes progression of preinvasive breast cancer: myoepithelial expression of $\alpha (v)\beta 6$ integrin in DCIS identifies high-risk patients and predicts recurrence. *Clin Cancer Res* 2014; **20**: 344–357.
42. Westcott JM, Precht AM, Maine EA, *et al.* An epigenetically distinct breast cancer cell subpopulation promotes collective invasion. *J Clin Invest* 2015; **125**: 1927–1943.

SUPPLEMENTARY MATERIAL ONLINE**Supplementary figure legends**

Figure S1. Frequency histogram for the integrin α 11 staining index

Figure S2. Integrin α 11 expression in spindle-shaped cells in the stroma of invasive human breast carcinomas by IHC

Figure S3. Intratumor heterogeneity of stromal integrin α 11 expression in human invasive breast cancer

Figure S4. Survival curves across molecular subtypes according to stromal integrin α 11 protein expression

Figure S5. Survival curves across molecular subtypes according to integrin α 11 mRNA expression in the METABRIC discovery dataset

Figure S6. Survival curves across molecular subtypes according to integrin α 11 mRNA expression in the METABRIC validation dataset